Eighth International Conference on
THIN-WALLED STRUCTURES – ICTWS 2018
Lisbon, Portugal, July 24-27, 2018

# BUILT-UP COLD-FORMED STEEL BEAMS USING RESISTANCE SPOT WELDING: EXPERIMENTAL INVESTIGATIONS

**Viorel Ungureanu*, Ioan Both*, Mircea Burca**, Marius Grosan*, Calin Neagu* and Dan Dubina***

* Politehnica University of Timisoara, Department of Steel Structures and Structural Mechanics
e-mails: viorel.ungureanu@upt.ro, ioan.both@upt.ro, calin.neagu@upt.ro, dan.dubina@upt.ro

** Politehnica University of Timisoara, Department of Materials and Manufacturing Engineering
e-mail: mircea.burca@upt.ro

**Keywords**: Built-up beams; Cold-formed steel members; Corrugated web; Resistance spot welding; Experimental tests; Galvanized steel.

**Abstract**. *The advances in cold-formed steel built-up elements require not only material savings but also high efficiency of production and manpower reduction. The WELLFORMED research project, ongoing at the CEMSIG Research Center of the Politehnica University of Timisoara, proposes to study a new technological solution for built-up beams made of corrugated steel sheets for the web and thin-walled cold-formed steel profiles for the flanges, connected by spot welding. Within the research project, the experimental work includes tensile-shear tests on the lap joint spot-welded specimens, were different combinations of steel sheets with various thicknesses were tested and, tests on full scale beams in bending. The study intends to demonstrate the feasibility of the proposed solutions, to assess their performance and to enlarge the knowledge by using numerical simulations for the optimization of the current solution and to define the limits of the solution's applicability.*

## 1 INTRODUCTION

Built-up steel beams, with sinusoidal or trapezoidal corrugated webs, represent a relatively new structural system that has been developed in the last two decades, especially in Germany and Austria. An increased interest for this solution was observed for the mainframe of single storey buildings and steel bridges, respectively. The main advantage of this type of element is the effect of the corrugation in stability problems, leading to increased buckling resistance, with a more economical design. The use of thinner materials leads to lower costs for materials, saving 10-30% compared to conventional welded beams and over 30% compared to hot-rolled ones. The height of a common sinusoidal corrugated steel sheet used as web is comparable to a 12 mm thick flat sheet or more. In the solutions developed so far, the flanges are made of flat sheets, welded to the sinusoidal sheet for the web, involving a specific welding technology. For these elements, the flanges provide the main bending resistance, with a small contribution of the sinusoidal corrugated web that offers shearing capacity. The design of corrugated web beams is included in Annex D of EN 1993-1-5 [1] together with the specific aspects covered by EN 1993-1-1 [2] and EN 1993-1- 3 [3].

A new technological solution of such a built-up beam, consisting of trapezoidal corrugated web and parallel flanges made of thin-walled cold-formed steel lipped channel sections, was developed within the CEMSIG Research Center (http://www.ct.upt.ro/en/centre/cemsig) of the Politehnica University of Timisoara [4,5], in which the connections between the flanges and the web were done by self-drilling screws. It is important to emphasize that the new solution, as a whole, is composed of 100% of cold-formed steel components, avoiding the

combination of two types of products, namely cold-formed elements for the web and hot-rolled for the flanges.

The technical solution presented above [4] was also extended for trapezoidal steel beams [6]. In the latter case, experimental tests were carried out on two beams with a 12 m span, with different connection arrangements between the flanges and the web.

A detailed state-of-the-art regarding built-up beams using cold-formed steel elements, was presented in [4,5].

A very important aspect related to the cold-formed steel components or structures is the connecting technique.

In order to meet the high standards of the automotive industry, new welding processes have been developed that further push the physical and mechanical limits of welding technology. Fronius is the market leader in the field of robotic welding systems, with more than 50 years of experience in the automotive and components supply industry. These technologies, due to their advantages, have also begun to be used in the steel structure domain. Among these technologies, one can notice: (1) Cold Metal Transfer (CMT) welding, that guarantees the most stable electric arc in the world and precise control of the process, offering welded bead and soldering without welding drops, and able to weld thicknesses from 0.6 mm; (2) Laser hybrid welding, combining the advantages of a fully digital MIG/MAG process with those of laser welding in a single process, but without their disadvantages. This allows the automatic joining of various steel parts at a speed of up to 8 meters per minute with high quality connection; (3) Resistance spot welding, a technique for joining of two or more sheets, by Joule-Lenz effect, without additional material. In the welding area, with the use of two copper alloy electrodes, a compressive force is applied and a high electric current is transmitted, which locally heats the parts, by Joule-Lenz effect, in a very short time. Thus, the material between the electrodes, at the interface of the contact zone between sheets is melted under the form of melted nucleus and after the welding current has stopped, the materials solidify and the joint results, creating a welded spot.

Briskham et al. [7] performed a comparative study on self-pierce riveting, resistance spot welding and spot friction joining, identifying the resistance spot welding as a more favourable option.

Guenfoud et al. [8] tested welded specimens fabricated through one, two or four layers of thin steel sheets using the shear resistance and tension resistance of multi-layer arc spot welds.

Snow [9] conducted a research in order to establish a relationship between electric arc spot weld shear strength and the arc time used while forming the weld. Testing was performed on steel gauge sheets of 0.85 mm, 1 mm, 1.3 mm and 1.6 mm. Each gauge material was tested in single-, double- and four-layer configurations. The research has proven that arc time has a tremendous influence on arc spot weld shear strength.

Strength tests were performed by Chao [10] to reveal the failure mechanisms of spot weld in lap-shear and cross tension test samples. Based on the observed failure mechanism, stress distribution was assumed. A theoretical model was developed to the mixed normal/shear loading condition.

In [11], finite element modelling and fracture mechanics calculations were used to predict the resistance spot weld failure mode and loads in shear-tension tests of advanced high-strength steels. The results of the work confirmed the existence of a competition between two different types of failure modes, namely full button pull-out and interfacial fracture. The study indicates that the load-bearing capacity of the welds is not affected by the fracture mode. Therefore, the mode of failure should not be the only criteria used to judge the quality of spot

welds. The load-bearing capacity of the weld should be the primary focus in the evaluation of the shear-tension test results.

Miyazaki and Furusako [12] investigate the dependency of fracture position and maximum load of laser welded lap joints through tensile shear test of joints, and a mechanical prediction model for the test results was developed.

Research progresses on arc welding techniques are described by Kodama et al. [13], focusing on the automotive members. Static strength and fatigue strength performance of welded joints are improved for high-strength steels by CMT applied arc spot welding.

In [14], low carbon steel plates, joined by friction stir spot welding (FSSW) with lap configuration were investigated. It was found the tool penetration depth exerted a strong effect on the failure mode of the joined samples and a weak effect on the joint shear strength. With increasing tool penetration depth, and with increasing depth of the tool shoulder pressing into the top sample, the failure mode in a lap-shear test changed from brittle to ductile and concentrated near the pinhole located away from the weld towards the base metal.

A wide experimental investigation on laser welded connections based on both lap-shear and tension tests were performed by Landolfo et al. [15].

Rusinski et al. [16] present selected problems which emerged from axial compression tests of thin-walled beams joined by spot welding. They investigate the effect of the size of the diameter of the weld and the pitch of the weld on the amount of absorbed energy. A discrete model was built and FEM strength computations of the thin-walled beams, taking into account physical and geometrical nonlinearities, were performed.

For resistance spot welding, in order to adopt a proper technology, it is impetuous necessary to have an equipment that may control the parameters of the welding i.e. force, time, current while the user needs to pay attention to the electrode tip diameter, since the thickness of the welded sheets varies and these 4 variables influence the resistance spot weld [17].

The study done by Pouranvari et al. [18] lead to an analytical model to predict the failure mode of resistance spot welds. However, metallurgical characteristics of welds should be considered to predict and analyse the spot weld failure mode more precisely.

Investigations on materials different from the steel sheets, e.g. stainless steel, which are connected by spot welding, are also performed in [19,20].

The paper presents the results of the experimental program performed on small specimens, tensile-shear tests on the lap joint spot-welded specimens, and on full scale built-up beams of corrugated web beams and cold-formed steel profiles as flanges, connected by using spot welding.

## 2 FROM TENSILE-SHEAR TESTS TO FULL SCALE TESTS

In the CEMSIG Research Center is currently carrying out the WELLFORMED research project, funded by the *Executive Agency for Higher Education, Research, Development and Innovation Funding* (UEFISCDI), which proposes a new connecting solution, namely spot welding, to be used for built-up cold-formed steel beams having the cross-section made of corrugated steel webs and flanges made of thin-walled cold-formed steel profiles.

The research project involves a large experimental program on tensile-shear tests on the lap joint spot-welded specimens, were different combinations of steel sheets with various thicknesses were tested, and tests on full scale beams, to demonstrate the feasibility of the proposed solutions, to assess their performance and to enlarge the knowledge by using

numerical simulations for the optimization of the current solution and to define the limits of applicability of the solution by parametric studies.

This new solution can be used as steel supporting framework in building construction: as roof girders, portal and low rise multi-story frames, short span pedestrian bridges. Also, it can be a reliable alternative to purlins or secondary beams, where these have to cover large bays. It is expected from this solution to cover spans up to 24 m length.

The proposed new solution is based on an experimental program previously developed within the CEMSIG Research Center, in which five corrugated web beams with flanges of back-to-back cold-formed lipped channel steel profiles were tested, having a span of 5157 mm and a height of 600 mm, with different arrangements/configurations for the self-drilling screws position and for the additional shear panels as shown in [4,5].

As presented in the previous section, spot welding is a feasible technique for connecting two or more sheets, without additional material. The weld is created by two copper alloy electrodes, which transmit a compressive force and electric current. By the heat developed at the interface of the contact zone between the sheets, the material is melted and after the welding current has stopped, the materials solidify creating a welded spot.

In order to fully investigate the response of full scale built-up beams connected by spot welding, the experimental tests comprised: a) tensile-shear tests on lap joint spot-welded specimens with various thickness combinations, b) tensile tests on base material and c) full scale tests on built-up beams in bending.

### 2.1 Tensile-shear tests on lap joint spot-welded specimens

To understand the behaviour of the built-up beams made of corrugated web beams and cold-formed steel profiles as flanges, connected by using spot welding, and for the characterisation of the behaviour of all types of connections, tensile-shear tests on lap joint spot-welded specimens have been performed.

The combinations between different sheet thicknesses, experimentally tested, are shown in Table 1. The notations $t_1$ and $t_2$ represent the thicknesses of the steel sheets in the connection and $d_s$ is the diameter of the spot welding. The diameter of the spot welding, $d_s$, was determined according to EN 1993-1-3 [3] for the case of resistance welding, i.e. $d_s = 5\sqrt{t}$, where $t$ is the smallest thickness of the connected steel sheets. A total number of 140 specimens were tested. The dimensions of the specimens, generically represented in Figure 1, were chosen in accordance with the specifications given in Chapter 8.4 of EN 1993-1-3 [3]. According to EN 1993-1-3 [3], all specimens were connected using one spot of welding. The specimens have been produced using Inverspotter 14000 Smart Aqua equipment from Telwin company, able to control the variables of a spot welding as: welding current, welding time and force between the electrodes in Smart Auto Mode.

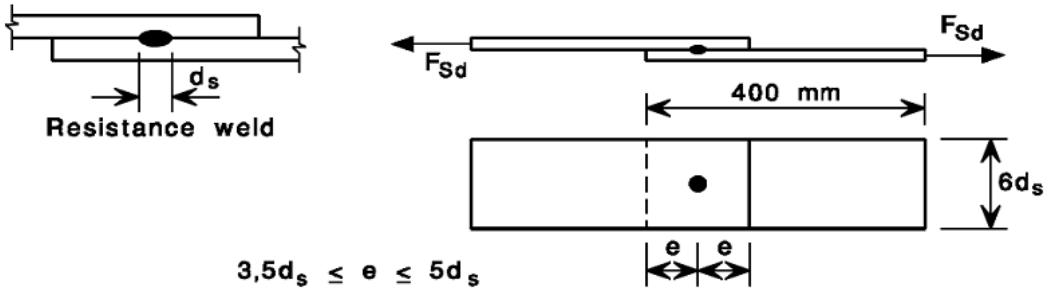


Figure 1: The dimensions of the specimens according to EN 1993-1-3 [3].

It should be mentioned that a similar experimental program, but focused on 0.7 and 0.8 mm thicknesses only, was performed by Benzar et al. [21] at the CEMSIG Research Center. The above sheet thickness combinations only concerned the connection of corrugated steel sheets of the web, to ensure the continuity of the web.

Table 1: Types of spot welding specimens (one spot of welding per specimen).

| Name | $t_1$ [mm] | $t_2$ [mm] | $d_s$ [mm] | No. of tests |
|---|---|---|---|---|
| SW-0.8-0.8 | 0.80 | 0.80 | 4.5 | 7 |
| SW-0.8-1.0 | 0.80 | 1.00 | 4.5 | 7 |
| SW-0.8-1.2 | 0.80 | 1.20 | 4.5 | 7 |
| SW-0.8-1.5 | 0.80 | 1.50 | 4.5 | 7 |
| SW-0.8-2.0 | 0.80 | 2.00 | 4.5 | 7 |
| SW-0.8-2.5 | 0.80 | 2.50 | 4.5 | 7 |
| SW-1.0-1.0 | 1.00 | 1.00 | 5.0 | 7 |
| SW-1.0-1.2 | 1.00 | 1.20 | 5.0 | 7 |
| SW-1.0-1.5 | 1.00 | 1.50 | 5.0 | 7 |
| SW-1.0-2.0 | 1.00 | 2.00 | 5.0 | 7 |
| SW-1.0-2.0 | 1.00 | 2.50 | 5.0 | 7 |
| SW-1.2-1.2 | 1.20 | 1.20 | 5.5 | 7 |
| SW-1.2-1.5 | 1.20 | 1.50 | 5.5 | 7 |
| SW-1.2-2.0 | 1.20 | 2.00 | 5.5 | 7 |
| SW-1.2-2.5 | 1.20 | 2.50 | 5.5 | 7 |
| SW-1.5-1.5 | 1.50 | 1.50 | 6.1 | 7 |
| SW-1.5-2.0 | 1.50 | 2.00 | 6.1 | 7 |
| SW-1.5-2.5 | 1.50 | 2.50 | 6.1 | 7 |
| SW-2.0-2.0 | 2.00 | 2.00 | 7.1 | 7 |
| SW-2.0-2.5 | 2.00 | 2.50 | 7.1 | 7 |

Experimental tests were conducted using the UTS universal testing machine. The distance between the sensors of the extensometer was 80 mm. Figure 2 shows a tested specimen with one spot welding of the SW-1.2-1.5 set, developing the full button pull-out failure.

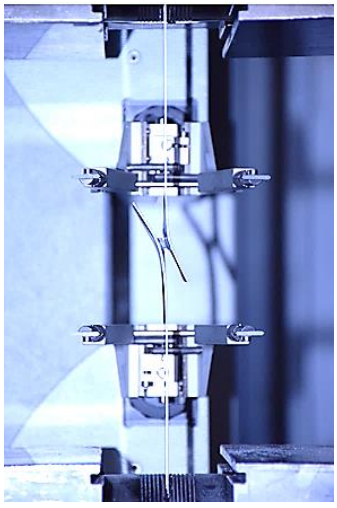

Figure 2: Full button pull-out failure mode.

Another important aspect of the investigation was the welding regime. The welding equipment has default factory settings counting for different thickness combinations, the so-called "SMART AUTO" setting, but also allows the possibility to use user-defined programs. Table 2 shows, as an exemplification, the parameters analysed for the set of SW-1.2-1.5 specimen.

Table 2: Welding regimes for the set SW-1.2-1.5.

| | Name | $I_s$ [A] | Power [%] | $F$ [daN] | Air pressure [bar] | $t_s$ [ms] |
|---|---|---|---|---|---|---|
| REG 1 | SW-1.2-1.5-1 | 10366 | 70 | 365 | 6 | 380 |
| REG 2 | SW-1.2-1.5-2 | 10336 | 70 | 365 | - | 380 |
| REG 3 | SW-1.2-1.5-3 | 11088 | 75 | 483 | 6.8 | 600 |
| REG 4 | SW-1.2-1.5-4 | 11088 | 75 | 472 | 6.6 | 600 |
| REG 5 | SW-1.2-1.5-5 | 11055 | - | 457 | 6.4 | 600 |
| REG 6 | SW-1.2-1.5-6 | 11775 | 80 | 449 | 6.2 | 600 |

The following parameters were considered: welding current $I_s$ (A), force between the electrodes $F$ (daN), air pressure (bar) and welding time, $t_s$ (ms), for electrodes of 13 mm diameter and 32 mm radius of the tip.

Figure 3 shows the set of the six SW-1.2-1.5 specimens with the parameters shown in Table 2, before and after testing. It can be noticed that in all cases the failure mode was the full button pull-out.

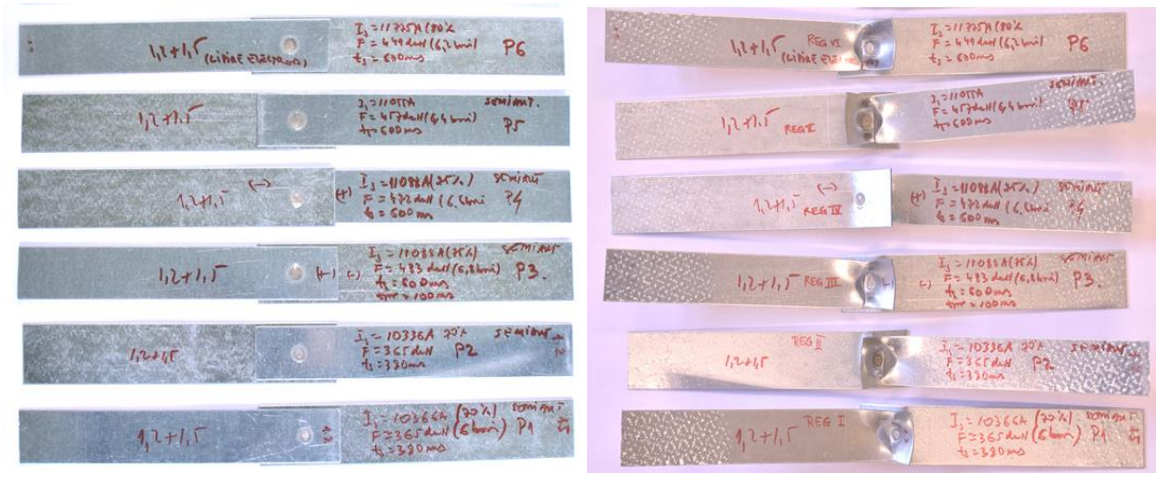

Figure 3: Specimens SW-1.2-1.5 before and after testing, using different welding regimes.

Figure 4 depicts the comparison of the force-displacement curves for the specimen set presented above, using different welding regimes. It can be seen that the specimens have a very good capacity and ductility, the maximum recorded force exceeding 12 kN.

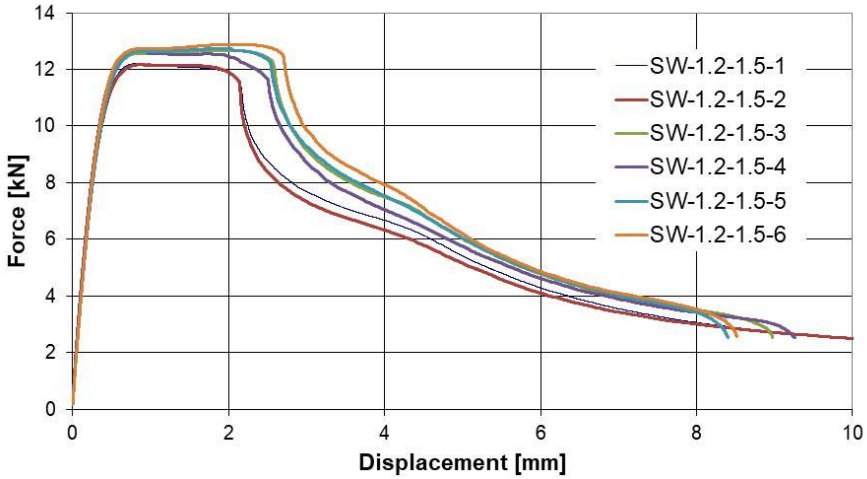


Figure 4: Force-displacement curves for SW-1.2-1.5 specimens (one spot of welding).

Performing the tests on all the specimens presented in Table 1, the general conclusion that can be drawn is that both the capacity and the ductility of the tested specimens are very good. Moreover, compared to the same specimens tested using self-drilling screws [4,5], the capacity of the tested specimens is double, but the ductility is decreased.

The tests revealed two types of failure modes, i.e. full button pull-out (nugget pull-out) and interfacial fracture (see Figure 5). For the investigated combinations of thicknesses, most of them failed by full button pull-out, as shown in Table 3.

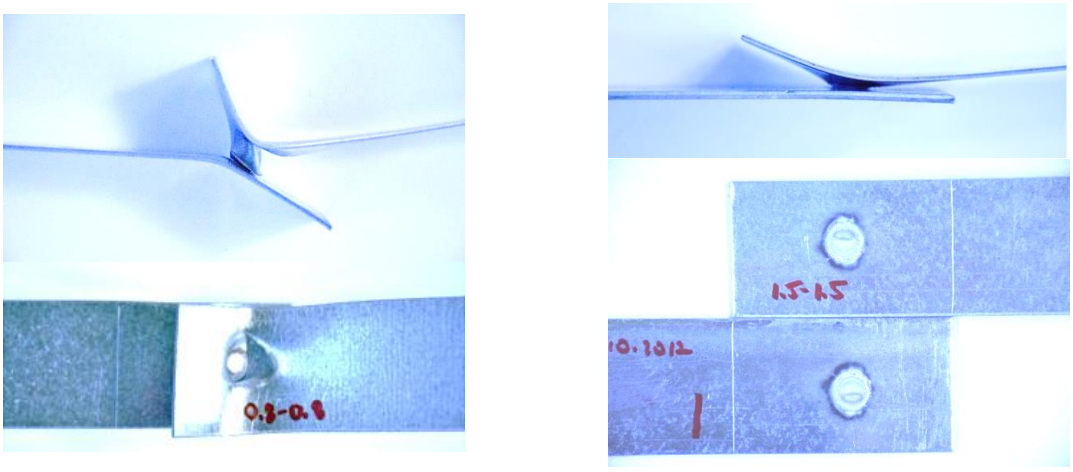

a) b)

Figure 5: Failure modes of the spot welding specimens: a) full button pull-out, b) interfacial fracture.

Table 3: Measured dimensions and failure modes for the SW specimens (see Figure 1 for dimensions).

| Specimen | min($t$) (mm) | $d_{s.measured}$ (mm) | $b = 6\,d_s$ (mm) | $e$ (mm) | Failure mode |
|---|---|---|---|---|---|
| SW-0.8-0.8 | 0.80 | 5.10 | 27.02 | 19.92 | Nugget pull-out |
| SW-0.8-1.0 | 0.81 | 5.10 | 27.30 | 20.60 | Nugget pull-out |
| SW-0.8-1.2 | 0.80 | 5.30 | 27.76 | 20.64 | Nugget pull-out |
| SW-0.8-1.5 | 0.80 | 5.50 | 27.47 | 20.45 | Nugget pull-out |
| SW-0.8-2.0 | 0.80 | 5.50 | 27.74 | 21.41 | Nugget pull-out |
| SW-0.8-2.5 | 0.79 | 6.00 | 27.57 | 21.38 | Nugget pull-out |
| SW-1.0-1.0 | 0.99 | 5.40 | 30.48 | 25.15 | Nugget pull-out |
| SW-1.0-1.2 | 1.00 | 5.40 | 30.48 | 27.54 | Nugget pull-out |
| SW-1.0-1.5 | 1.01 | 5.50 | 30.69 | 25.42 | Nugget pull-out |
| SW-1.0-2.0 | 1.01 | 6.00 | 30.85 | 26.31 | Nugget pull-out |
| SW-1.0-2.5 | 1.01 | 6.20 | 30.60 | 27.73 | Nugget pull-out |
| SW-1.2-1.2 | 1.19 | 5.60 | 33.13 | 24.70 | Nugget pull-out |
| SW-1.2-1.5 | 1.21 | 5.80 | 33.07 | 26.00 | Nugget pull-out |
| SW-1.2-2.0 | 1.21 | 6.00 | 33.46 | 27.55 | Nugget pull-out |
| SW-1.2-2.5 | 1.20 | 6.40 | 33.33 | 27.23 | Nugget pull-out |
| SW-1.5-1.5 | 1.53 | 6.50 | 37.24 | 29.75 | Interfacial fracture |
| SW-1.5-2.0 | 1.54 | 7.00 | 37.32 | 31.00 | Nugget pull-out |
| SW-1.5-2.5 | 1.52 | 7.50 | 37.48 | 31.57 | Nugget pull-out |
| SW-2.0-2.0 | 1.99 | 7.50 | 42.15 | 36.28 | Interfacial fracture |
| SW-2.0-2.5 | 1.97 | 7.80 | 42.61 | 35.99 | Interfacial fracture |

In the full button pull-out, the fracture occurs in the base metal or in the perimeter of the weld. In this failure mode, the material is completely torn from one of the sheets with the weld remaining intact. This is the most common failure mode for the tested specimens.

Another type of failure mode is the interfacial fracture in which the weld fails at the interface of the two sheets, leaving half of the weld nugget in one sheet and half in the other.

As a conclusion, in the case of full button pull-out, the strain in the base material outside the weld nugget is greater than the strain developed at the weld interface and the opposite is true for the case of the weld interfacial failure. In addition, from the experimental results, it is noticed that the load-bearing capacity of the weld is not affected by the fracture mode.

The quantitative results, in terms of force and displacements, are presented in Figure 6.

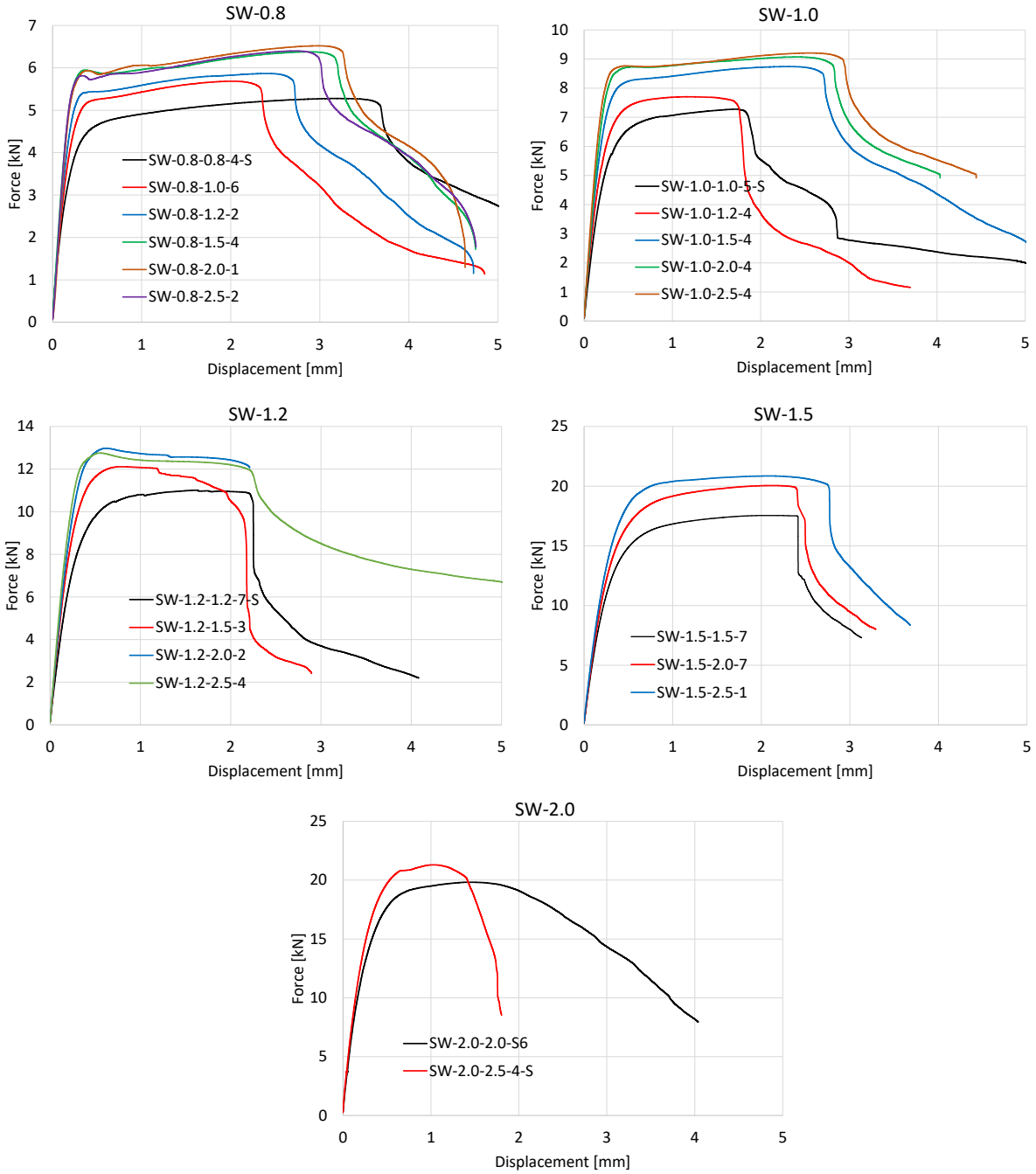


Figure 6: Response of simple SW specimens.

It may be observed that for each combination the maximum force is not limited by the minimum thickness, as the force increases if a smaller thickness is connected to a thicker

sheet, but it exists an upper limit of the bearing capacity of the welded connection which is the equivalent of a plastic force of the smaller thickness.

### 2.2 Tensile tests

Specimens of all the sheet thicknesses that were involved in the built-up beams, i.e. 0.8 mm, 1.0 mm, 1.2 mm, 1.5 mm, 2.0 mm and 2.5 mm were prepared for tensile tests with the nominal width of 20 mm. A number of 5 specimens for each thickness was considered.

The mechanical characteristics of the base material were obtained according to the international standard ISO 6892-1, Metallic materials - Tensile testing - Part 1: Method of test at room temperature [22]. Experimental tests were conducted using the UTS universal testing machine. Figure 7 presents one specimen of each thickness before and after testing.

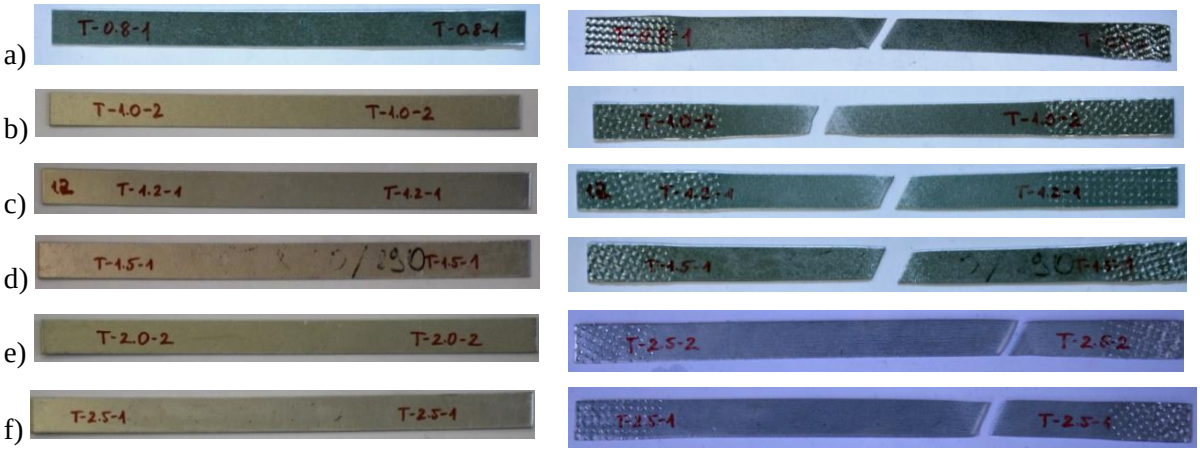


Figure 7: Tensile test specimens – before and after test
a) t = 0.8 mm, b) t = 1.0 mm, c) t = 1.2 mm, d) t = 1.5 mm, e) t = 2.0 mm, f) t = 2.5 mm.

The tensile tests revealed the stress-strain relationships for each thickness. The specimens for 1.2, 1.5 and 2.0 mm showed a classic yield plateau as shown in Figure 8(a), while the specimens for 0.8, 1.0 and 2.5 mm have a reduced plateau, as presented in Figure 8(b).

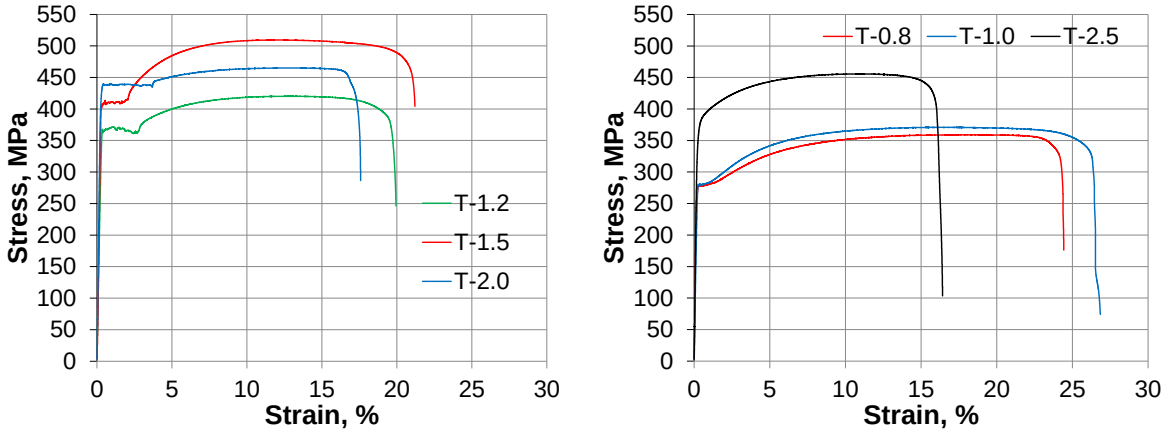


a) b)

Figure 8: Stress-strain relationships.

The curves presented in Figure 8 represent a selection from the tests, while the mean values of the tests per each thickness are given in Table 4.

Table 4: Material properties.

| $t$ (mm) | $R_{p0.2}$ (MPa) | $R_{eH}$ (MPa) | $R_m$ (MPa) | $A_g$ % | $A_{gt}$ % | $A_t$ % |
|---|---|---|---|---|---|---|
| 0.8 | 279.64 | 282.67 | 361.76 | 18.23 | 18.41 | 26.60 |
| 1.0 | 281.33 | - | 373.50 | 16.40 | 16.70 | 26.14 |
| 1.2 | 366.82 | 367.81 | 420.68 | 12.77 | 13.15 | 19.83 |
| 1.5 | 407.70 | 409.00 | 497.12 | 12.80 | 13.06 | 20.38 |
| 2.0 | 431.78 | 430.43 | 464.46 | 11.55 | 11.79 | 19.70 |
| 2.5 | 374.68 | - | 452.98 | 11.16 | 11.40 | 16.76 |

where:
$R_{p0.2}$ stress at 0.2% strain
$R_{eH}$ maximum value of stress prior to the first decrease in force
$R_m$ stress corresponding to the maximum force
$A_g$ plastic extension at maximum force
$A_{gt}$ total extension at maximum force
$A_t$ total extension at the moment of fracture

## 2.3 Full scale beam specimen tests

For the full-scale specimen tests, two beams were built-up, i.e. CWB SW-1 and CWB SW-2, having a span of 5157 mm and a height of 600 mm. The process for the manufacturing consists of 4 steps: a) connecting the corrugated steel sheets for the web, b) connecting the shear panels at the ends of the beam, c) connecting the top and bottom flanges and d) connecting the end parts of the beam for the rigid connection to the experimental stand, as presented in Figure 9. The first step in only necessary if the corrugated web is not available in one piece. For the current case, the corrugated steel sheets had a maximum length of 1.05 m.

a)

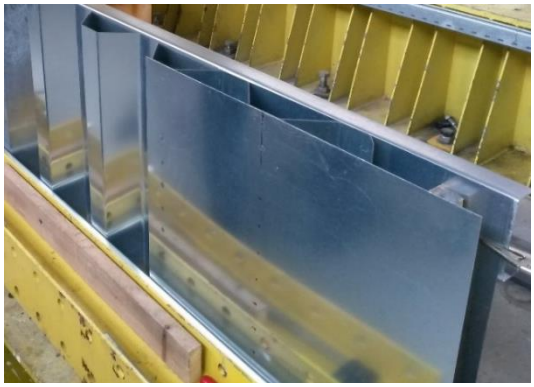

b)

c)

d)

Figure 9: Stages of beam built-up.

The components of the built-up beams are shown in Figure 10 and detailed below:
- two back-to-back lipped channel sections for flanges - 2 × C120/2.0;
- corrugated steel sheets (panels of 1.05 m length with 0.8 mm and 1.2 mm thicknesses);
- additional shear panels - flat plates of 1.0 or 1.2 mm;
- reinforcing profiles U150/2.0 used under the load application points;
- bolts M12 grade 8.8 for flange to endplate connection.

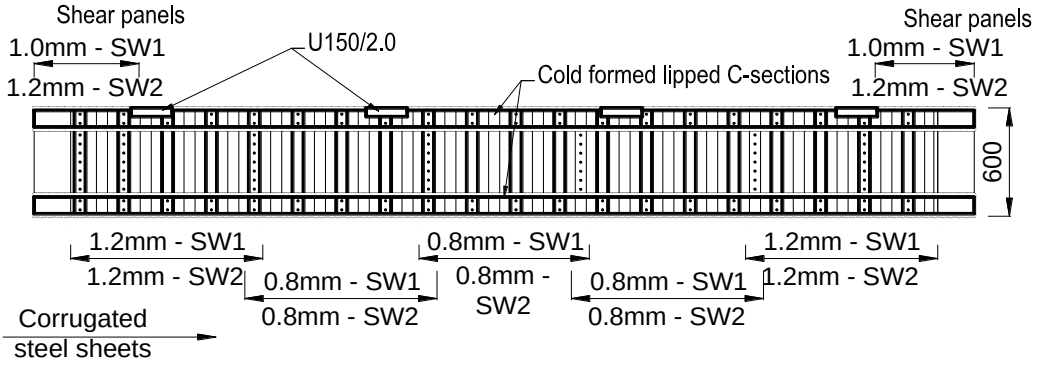


Figure 10: Components of the built-up beams.

The details concerning the connections of the beam are: (1) spot welding for the overlapping of corrugated steel sheets; (2) spot welding for the connection between the corrugated steel sheet and shear panels; (3) spot welding between the flanges and the corrugated web (4) spot welding between the shear panels and the flanges; (5) connection between the shear plates and the end support, M12 gr 8.8 bolts; and (6) connection between the flanges and the end supports, M12 gr 8.8 bolts.

Except the differences between the shear panel's thicknesses of the two beams, as shown in Figure 10 and Table 5, another aspect of interest was the connection between the corrugated steel sheets of the web. By using the same number of spot welds, the corrugated sheets of beam CWB SW-1 were connected on two rows (Figure 11(a)), while the corrugated sheets of beam CWB SW-2 were connected on one row only as shown in Figure 11(b).

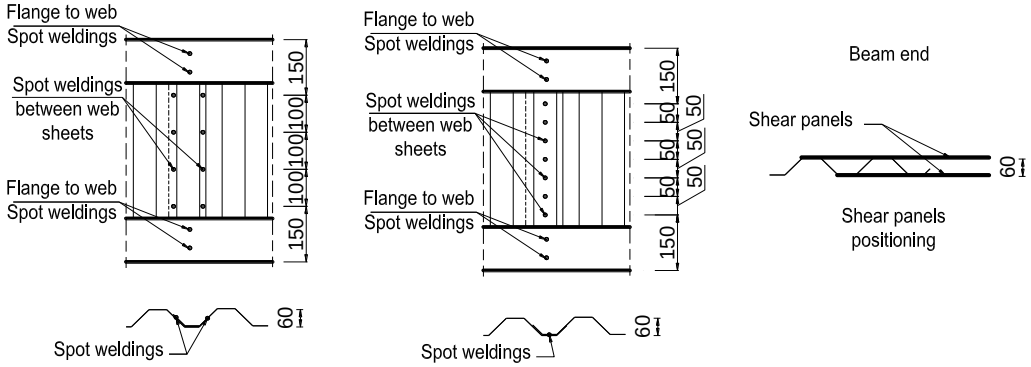


a) b) c)

Figure 11: a) Connection between corrugated sheets of beam CWB SW-1,
b) Connection between corrugated sheets of beam CWB SW-2, c) position of the shear panels.

Table 5: Distribution of the steel sheets used for the web of the spot-welded beams.

| Name | Thickness | | | Length of shear panels* |
|---|---|---|---|---|
| | Outer corrugated sheets | Inner corrugated sheets | Shear panels | |
| CWB SW-1 | 1.2 mm | 0.8 mm | 1.0 mm | 470 mm; 570 mm |
| CWB SW-2 | 1.2 mm | 0.8 mm | 1.2 mm | 510 mm; 630 mm |

* the length of the shear panels is different due to variable position of the web corrugation

Finally, the beams with the configuration and the details presented in Figure 12(a), were loaded in a 2D loading frame, with the test set-up depicted in Figure 12(b). The beams were loaded by an actuator of 500 kN which transmitted the force to the beam by a system able to distribute the load in 4 points. An out-of-plane independent frame was used to avoid stability problems during loading.

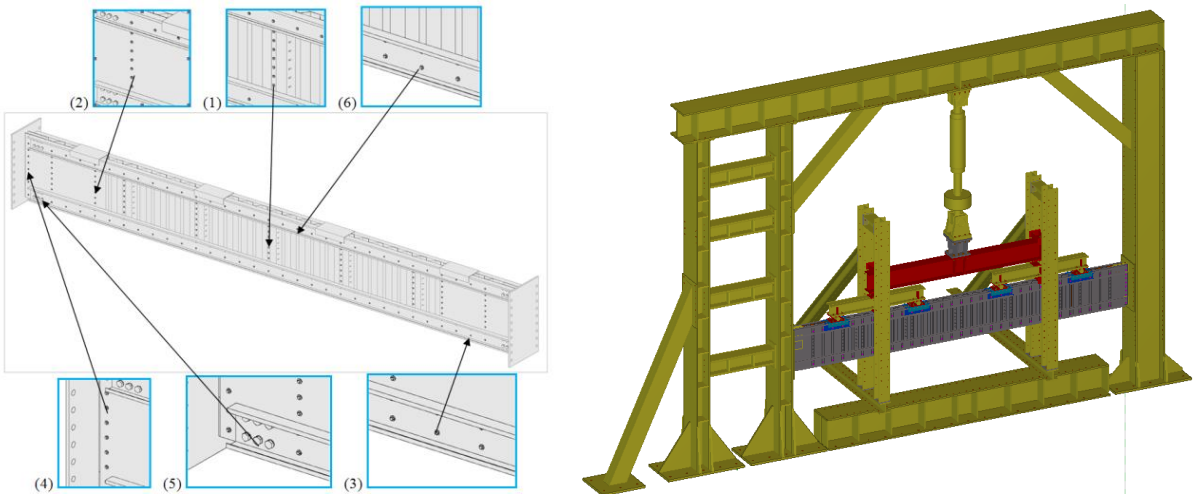


a) b)

Figure 12: a) Type and position of the connections used for the spot-welded beams, b) Test setup.

The recordings aimed to monitor the displacements at each end of the top or bottom flange, between the flange and the end plate as well as between the end plate and the rigid frame, as shown in Figure 13(a). The vertical deflection of the beam was monitored at each quarter of the span by 2 wire displacement transducers connected to each of the bottom flange part (see Figure 13(b)). The force was recorded through the actuators load cell.

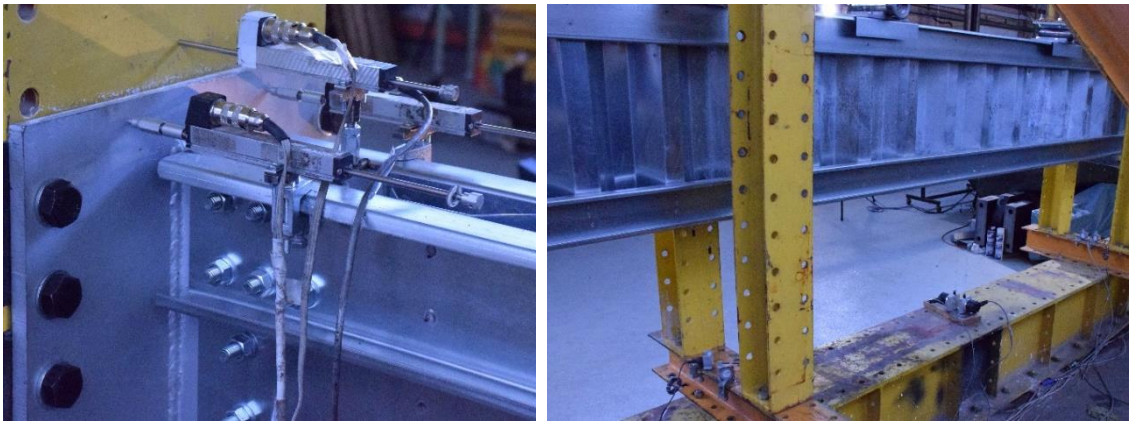

a) b)

Figure 13: a) Flange ends instrumentation, b) Vertical deflection instrumentation.

An optical monitoring system was used in order to assess the behaviour of the shear panels during loading. The shear panels were monitored using a digital image correlation system (DIC) provided by *isi-sys GmbH*. Two GT6600 Prosilica series of high resolution cameras (29 Mpix) with 35 mm lenses, recorded images for a 3D evaluation of the out of plane displacements and strain of the shear panel, at an acquisition frequency of 1 Hz.

The calibration process returned an average error of 0.038 pixels. A facet size (number of pixels per subset) and a step size (the spacing of the points that are analysed during correlation) of 10×10 and 5, respectively, were considered for an initial processing.

Figure 14 depicts the evolution during testing of the out of plane deformations (a, b, c) and the corresponding principal strains (d, e, f) of a given shear panel.

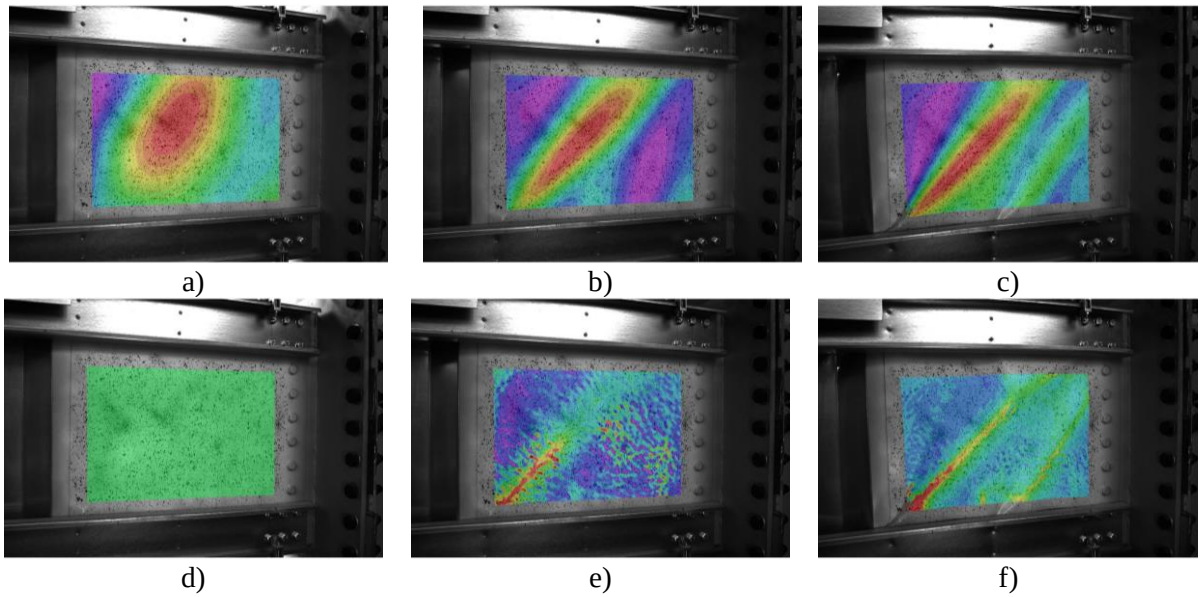


Figure 14: Evolution of the out of plane deformations (a, b, c) and the corresponding principal strains (d, e, f) of a given shear panel.

Although the strains at the beginning of the tests are null, the out-of-plane images recorded imperfections due to fabrication within the range of -1.4 mm and 2.0 mm. Also, two lines for the development of the maximum tensile strains are noticed on the shear panel area for that particular case.

## 3. RESULTS AND DISCUSSIONS

In the following, the remarks during the experiments are presented and discussed.

For the first tested specimen, CWB SW-1 (see Figure 15), the failure mode of the beam started with the buckling of shear panel (see Figure 16), followed by the distortions of the corrugated web as presented in Figure 17 and, after reaching the maximum force, the breaking of some spot-welding connections (see Figure 18). The behaviour of CWB SW-1 beam was ductile, with an initial stiffness of $K_{0\text{-}Exp}$ = 11352.6 N/mm and the maximum load was reached at $F_{max}$ = 283.8 kN. The collapse appears for a displacement of around 123 mm. The recorded force-displacement curve at the mid-span is depicted in Figure 23.


Figure 15: CWB-SW1 beam – global deformation during the testing.

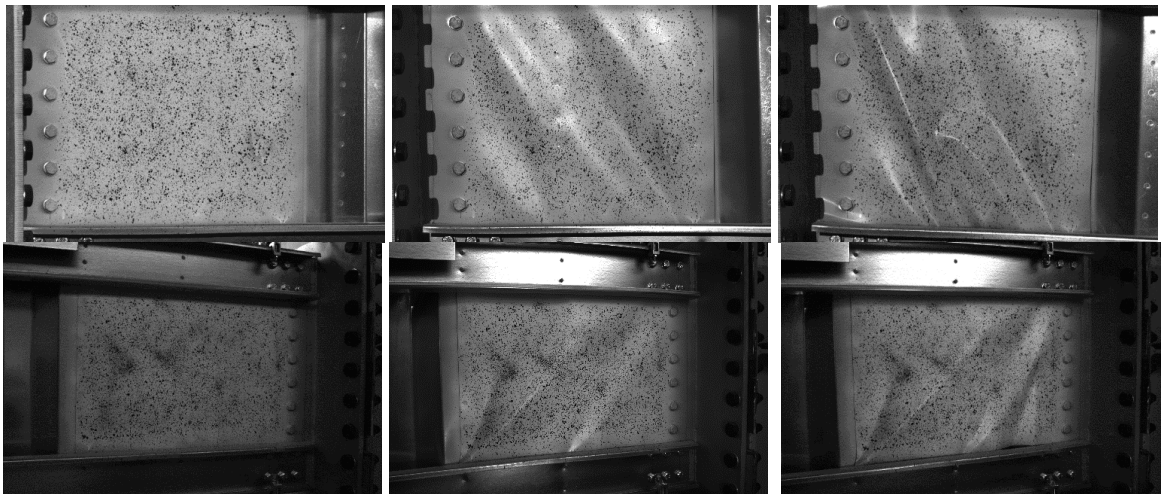

Figure 16: Development of the shear buckling at the end panels for CWB SW-1 beam.

Figure 16 presents some details of the web distortion. Due to the two connected points between the web and the flange (see Figure 11), under the shear stresses, the corrugations have been distorted between the two flanges with respect to the axis between the two spots of the welding.

Fig. 17. Distortion of the web corrugation of the CWB SW-1 beam.

Figure 18: Spot welding failure between the web and the flange- CWB SW-1 beam.

The second beam, CWB SW-2 (see Figure 19) presented a similar mechanism of failure, starting with the buckling of the shear panel (see Figure 20) at one end of the beam, followed by the distortions of the corrugated web as presented in Figure 21 and, after reaching the maximum force, the breaking of some spot-welding connections (see Figure 22). The behaviour was ductile, with an initial stiffness of $K_{0\text{-}Exp}$ = 15846.5 N/mm and the maximum capacity was achieved at $F_{max}$ = 276.0 kN. The collapse appears for a displacement of around 69.5 mm. The recorded force-displacement curve at the mid-span is depicted in Figure 23.


Figure 19: CWB SW-2 beam – global deformation during the testing.


Figure 20: Development of the shear buckling at the end panels for CWB SW-2 beam.

Figure 21: Distortion of the web corrugation of the CWB SW-2 beam.

Figure 22: Spot welding failure between the web and the flange - CWB SW-2 beam.

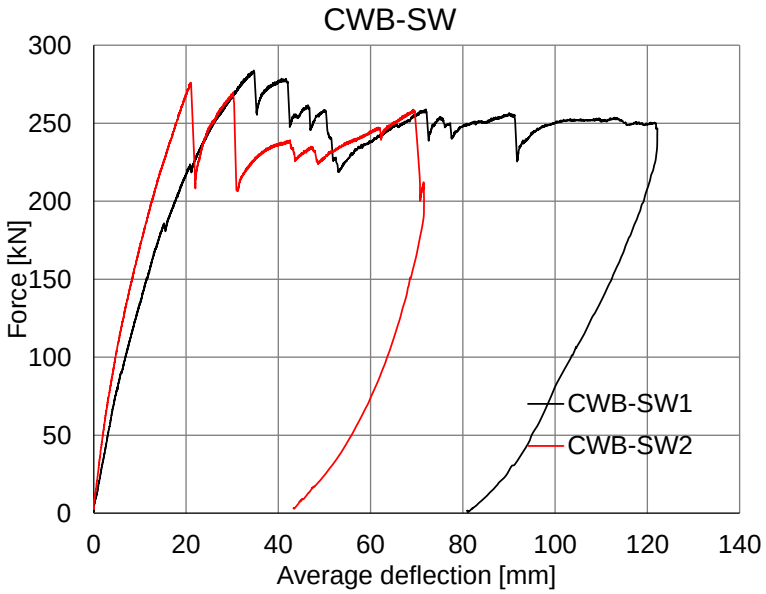


Figure 23: Force-deflection curve for the full scale built-up beams.

In the final stage of the tests, both beams exhibited local deformation under the load application points, as presented in Figure 24.

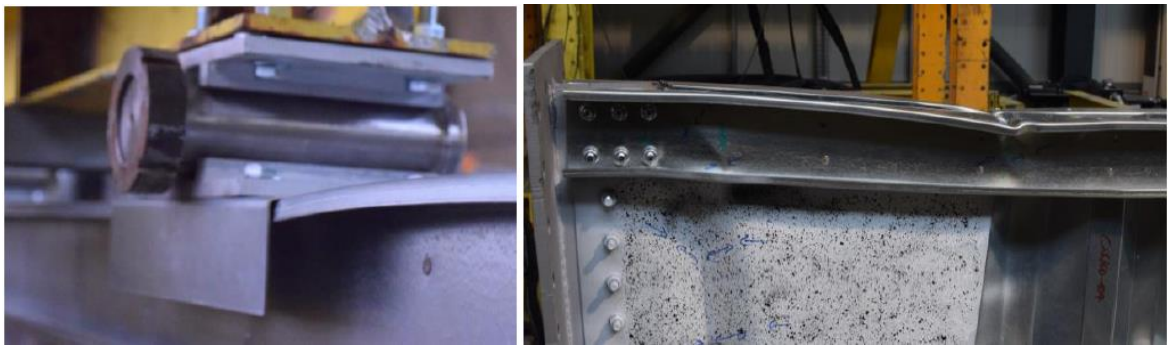

Figure 24: Local deformations under the load application point.

Compared to the previous studied solution, built-up beams with self-drilling screws [4,5], it may be seen that the beams connected by spot welding present a higher stiffness (see Table 6), as well as a higher capacity (see Figure 25).

Table 6. Results of the corrugated web beams: spot welding vs. screws.

| Beam type | $K_{0\text{-}Exp}$ (N/mm) | $F_{max}$ (kN) |
|---|---|---|
| CWB SW-1 | 11352.6 | 283.8 |
| CWB SW-2 | 15846.5 | 276.0 |
| CWB-1 [4,5] | 6862.2 | 219.0 |
| CWB-2 [4,5] | 7831.5 | 230.6 |
| CWB-3 [4,5] | 7184.9 | 211.9 |
| CWB-4 [4,5] | 3985.0 | 161.8 |
| CWB-5 [4,5] | 5516.2 | 215.5 |

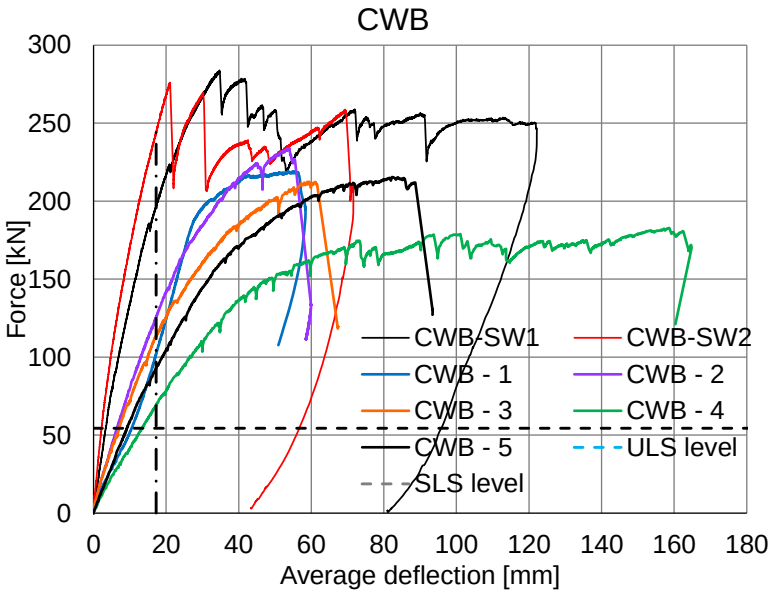


Figure 25: Force-displacement curve for the full scale built-up beams: spot welding vs. screws.

## 4 CONCLUSIONS

Within the WELLFORMED research project, carried out at the CEMSIG Research Center of the Politehnica University of Timisoara, an extensive experimental program on built-up cold-formed steel beams using resistance spot welding as connecting technology occurred.

The paper presents the experimental results on tensile-shear tests on lap joint spot-welded specimens, in order to characterize the behaviour of these connections and on full scale tests of two beams subjected to bending. The experiments were accompanied by tensile tests, to characterise the material behaviour.

The most common failure mode for the tensile-shear tests on lap joint spot-welded specimens was the full button pull-out. Also, can be noticed that for each combination of thicknesses, the maximum force is not limited by the minimum thickness; the force increases if a smaller thickness is connected to a thicker one, but exists an upper limit which is given by the plastic force of the smaller thickness. Both the capacity and the ductility obtained for the tested specimens are very good and compare to similar specimens tested using self-drilling screws [4,5], the capacity is double but the ductility is decreased.

The experimental results of full scale shown:

- both the capacity and the ductility obtained for the tested specimens are very good;
- compared to the solution studied in [4,5], they show an increased capacity but, the deformation is consistent less that the deformation of built-up beams using self-drilling screws.

The results are encouraging and demonstrate the potential of this solution for standardization and industrial manufacturing. Nevertheless, the experimental research will be followed by numerical simulations, to optimize the distribution/arrangement of the spot welding connections, and by parametric studies to see the suitability of such beams to larger spans and the limits of the system.

## ACKNOWLEDGEMENT

This work was supported by a grant of the Romanian National Authority for Scientific Research and Innovation, CNCS/CCCDI -UEFISCDI, project number PN-III-P2-2.1-PED-2016-1684 / WELLFORMED - *Fast welding cold-formed steel beams of corrugated sheet web*, within PNCDI III.

## REFERENCES


[1] EN 1993-1-5, *Eurocode 3: Design of steel structures - Part 1-5: Plated structural elements*, CEN, Brussels, 2006.

[2] EN 1993-1-1, *Eurocode 3: Design of steel structures - Part 1-1: General rules and rules for buildings*, CEN, Brussels, 2005.

[3] EN 1993-1-3, *Eurocode 3: Design of steel structures. Part 1-3: General Rules. Supplementary rules for cold-formed thin gauge members and sheeting*, CEN, Brussels, 2006.

[4] Dubina D., Ungureanu V. and Gîlia L., "Experimental investigations of cold-formed steel beams of corrugated web and built-up section for flanges", *Thin-Walled Structures* **90,** 159-170, 2015.

[5] Dubina D., Ungureanu V. and Gîlia L., "Cold-formed steel beams with corrugated web and discrete web-to-flange fasteners", *Steel Construction*, 6(2) (2013) 74-81.

[6] Nagy Zs., Ungureanu V., Dubina D. and Ballok R., "Experimental investigations of cold-formed steel trapezoidal beams of screwed corrugated webs", *Proc. of the International Colloquium on Stability and Ductility of Steel Structures - SDSS'2016*, Timisoara, Romania, 30/05-01/06, 387-394, 2016.

[7] Briskham P., Blundell N., Han L., Hewitt R., Young K. and Boomer D., "Comparison of self-pierce riveting, resistance spot welding and spot friction joining for aluminum automotive sheet", *SAE 2006 Congress*, Technical paper, 2006-01-0774, 2006.

[8] Guenfoud N., Tremblay R. and Rogers C.A., "Arc-Spot Welds for Multi-Overlap Roof Deck Panels", *Twentieth International Specialty Conference on Cold-Formed Steel Structures*, St. Louis, Missouri, USA, 3-4/11, 535-549, 2010.

[9] Snow G., "Strength of arc spot welds made in single and multiple steel sheets", *MsC Thesis*, Blacksburg, Virginia, USA, 2008.

[10] Chao Y.J., "Ultimate Strength and Failure Mechanism of Resistance Spot Weld Subjected to Tensile, Shear or Combined Tensile/Shear Loads", *Journal of Engineering Materials and Technology*, **125,** 125-132, 2003.

[11] Radakovic J. and Tumuluru M., "Predicting Resistance Spot Weld Failure Modes in Shear Tension Tests of Advanced High-Strength Automotive Steels", *Welding Journal*, **87,** 96-105, 2008.

[12] Miyazaki Y. and Furusako S., "Tensile Shear Strength of Laser Welded Lap Joints", *Nippon Steel Technical Report*, No. 95, 28-34, 2007.

[13] Kodama S., Ishida Y., Furusako S., Saito M., Miyazaki Y. and Nose T., "Arc Welding Technology for Automotive Steel Sheets", *Nippon Steel Technical Report*, No. 103, 83-90, 2013.

[14] Baek S.-W., Choi D.-H., Lee C.-Y., Ahn B.-W., Yeon Y.-M., Song K. and Jung S.-B., "Structure-Properties Relations in Friction Stir Spot Welded Low Carbon Steel Sheets for Light Weight Automobile Body", *Materials Transactions*, **51**(2), 399-403, 2010.

[15] Landolfo R., Mammana O., Portioli F., DiLorenzo G. and Guerrieri M.R., "Laser welded built-up cold-formed steel beams: Experimental investigations", *Thin-Walled Structures*, **46**(7-9), 781–91, 2008.

[16] Rusinski E., Kopczynski A. and Czmochowskia J., "Tests of thin-walled beams joined by spot welding", *Journal of Materials Processing Technology*, 157–158, 405–409, 2004.

[17] Jeffus L.F., *Welding: Principles and Applications*. C Delmar Publishers, Technology & Engineering, 1992.

[18] Pouranvari M., Marashi P., Goodarzi M. and Abedi A., An analytical model predicting failure mode of resistance spot welds", *Metal*, Hradec nad Moravicí, 13–15/5, 2008.

[19] Pouranvari M., Marashi P., Goodarzi M. and Abedi A., "Failure Mode Transition in AISI 304 Resistance Spot Welds, Welding Journal, **94**, 303-309, 2012.

[20] Darwish S. M., Soliman M. S. and AI-Fahead A. M., "Characteristics and Variables of Spot Welding and Weldbonding Bimaterials", *Materials and Manufacturing Processes*, **12** (2), 175-186, 1997.

[21] Benzar S., Ungureanu V., Dubina D. and Burca M., "Built-up cold-formed steel beams with corrugated webs connected with spot welding", *Advanced Materials Research*, **1111**, 157-162, 2015.

[22] EN ISO 6892-1, *Metallic materials - tensile testing. Part 1: Method of test at room temperature*, CEN, Brussels, 2009.